



## Self-Cleaning Cement Material with Bismuth Titanate Photocatalytic Additive

Irina Kozlova <sup>1</sup>, Marina Dudareva <sup>1\*</sup>, Olga Zemskova <sup>1</sup>, Andrey Korshunov <sup>1</sup>,  
Svetlana Samchenko <sup>1</sup>

<sup>1</sup> National Research Moscow State Civil Engineering University, 26, Yaroslavskoye Shosse, 129337 Moscow, Russia.

Received 19 July 2025; Revised 07 October 2025; Accepted 11 October 2025; Published 01 November 2025

### Abstract

Nowadays, mortars are building materials with various properties that can be achieved through the careful selection of components and the introduction of different modifying additives. An additive based on the  $\text{TiO}_2\text{--Bi}_2\text{O}_3$  oxide system can be considered a modifying component with photocatalytic and biocidal properties capable of decomposing organic pollutants, viruses, bacteria, and fungal spores. The purpose of the work was to obtain cement compositions containing the additive, study their physical and mechanical properties, evaluate their photocatalytic activity in accordance with the UNI 11259-2016 standard, and assess their resistance to mold fouling. In this study, samples of cement–sand plaster with the  $\text{TiO}_2\text{--Bi}_2\text{O}_3$  additive synthesized via citrate-based technology at 1.7 and 5.0 wt.% were prepared, and their physical, mechanical, photocatalytic, and biocidal properties were examined. As a result, the authors identified photocatalytic activity in both the UV and visible spectra, achieving 69% after 26 hours of UV irradiation. The samples demonstrated 100% resistance to mold fouling. The compressive strength of the modified samples increased by 32.0–39.0%; bending strength by 33–38.0%; and adhesion strength to the base by 60–70%. The cost calculation also confirmed the feasibility of introducing the additive at 1.7 wt.% into the cement composition. The resulting cement material formula can be recommended for designing fungi-resistant, self-cleaning plasters.

**Keywords:** Self-Cleaning Material; White Cement; Plasticizer; Photocatalysis; Fungi Resistance; Fine Additive;  $\text{TiO}_2\text{--Bi}_2\text{O}_3$  System.

## 1. Introduction

Since ancient times, building mortars have been widely used in construction for application on the surface of ceilings and walls as decorative and finishing coatings. Since Ancient Greece, clay, lime, and gypsum mortars have been used for leveling walls and ceilings, which later began to serve an artistic function: marble chips were added to the mortar to imitate the surface of natural stone, which also increased the strength of the coating. The introduction of mineral pigments into the plaster composition made it possible to create colored surfaces and decorative elements. The addition of aggregates with different granulometric compositions makes it possible to obtain textured coatings for interiors and building facades. To create expressive compositions, artists used painting with mineral-based pigments on raw and dried plaster. Nowadays, the range of plasters on the market is quite diverse. Modern finishing compositions are complex systems that include components of organic and inorganic origin and various chemical natures: binders, fillers, plasticizers, reinforcing additives to increase crack resistance, pigments, and antiseptic additives. Quartz sands and marble chips are used as fillers to create the effect of natural stone surfaces; mica and porous fillers (expanded polystyrene, vermiculite, perlite) are used to obtain warm and sound-insulating coatings. Some additives provide special properties to the coating: barite concentrate is introduced into the composition to obtain plasters that protect against

\* Corresponding author: [modudareva@yandex.ru](mailto:modudareva@yandex.ru)



<http://dx.doi.org/10.28991/CEJ-2025-011-11-014>



© 2025 by the authors. Licensee C.E.J, Tehran, Iran. This article is an open access article distributed under the terms and conditions of the Creative Commons Attribution (CC-BY) license (<http://creativecommons.org/licenses/by/4.0/>).

ionizing radiation, and photocatalysts provide self-cleaning ability to the surface due to the phenomenon of photocatalysis [1–3].

Photocatalysts are now promising objects for study and application in various fields of science and technology, from wastewater and air purification and filtration systems to photocatalytic water splitting for hydrogen production—a promising alternative source of clean “green” energy. In building materials science, photocatalysts can be incorporated into the mineral binder matrix, ceramic or glass structure for the manufacturing of plasters, façade panels, brick veneers, and cement pavement tiles. The use of paint and varnish products with a photocatalyst makes it possible to obtain self-cleaning façade elements of complex shapes. The self-cleaning effect is due to an oxidation–reduction process (Figure 1), in which adsorbed organic pollutants decompose under the influence of light into non-toxic photodegradation products. Its application can not only significantly reduce the cost of professional façade washing but can also purify the air. The concentration of volatile organic compounds (VOCs), car exhaust gases and industrial emissions, and nitrogen and sulfur oxides harmful to human health can be reduced by photocatalysis.

A photocatalytic process is initiated when a particle of a semiconductor photocatalyst is exposed to light. If the irradiation energy is sufficient, electrons in the semiconductor are transferred from the valence band to the conduction band, and then react with water and oxygen molecules to form reactive oxygen species (ROS) such as superoxide anion radical ( $\cdot\text{O}_2^-$ ), hydroxyl radical ( $\text{OH}\cdot$ ), and hydrogen peroxide ( $\text{H}_2\text{O}_2$ ) [4–12]. ROS formed during the photocatalysis process decompose surface contaminants and are also harmful to the spores of microscopic fungi, bacteria, and viruses, which positively affects the material’s ability to resist biofouling. Highly reactive radicals are able to interact with the cell membranes of fungi and bacteria, causing their destruction and death [13–16]. The most common photocatalysts introduced into building material structures are finely dispersed and nanoscale pure and doped metal oxides:  $\text{TiO}_2$ ,  $\text{Al}_2\text{O}_3$ ,  $\text{SiO}_2$ ,  $\text{ZnO}$ , and  $\text{Bi}_2\text{O}_3$ . These additives provide a photocatalytic effect and also improve the physical and mechanical characteristics of cement stone, such as strength and density [11–14], due to the promotion of hydration processes.

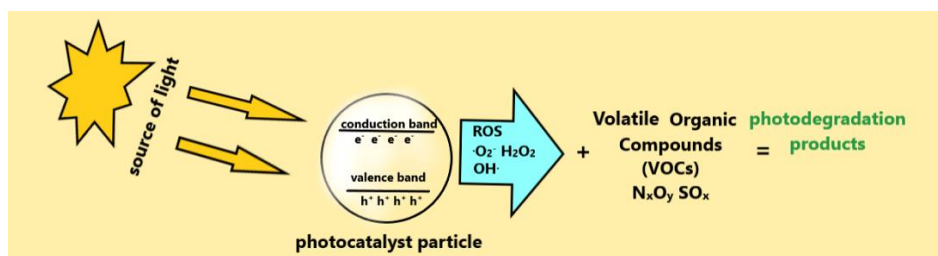


Figure 1. Photocatalysis process scheme

Despite the excellent photocatalytic qualities of well-known  $\text{TiO}_2$ ,  $\text{Bi}_2\text{O}_3$ , and  $\text{ZnO}$ , there are several main disadvantages—namely, their activity only in the UV spectral range and the rapid recombination of photogenerated charges. Therefore, scientists are developing new photocatalysts by modifying their structure with metal and nonmetal ions, as well as by creating complex hybrid heterostructures that would overcome these shortcomings. It is also necessary to expand the activity of photocatalysts into the visible part of the spectrum. In addition, there is always market demand for new additives, especially biocidal ones, because microorganisms’ resistance is constantly evolving [15–16]. Thus, researchers continue to investigate new photocatalytic compounds and biocidal additives. For example, photocatalytic bismuth-containing compounds and heterostructures—such as oxyhalides and layered bismuth titanates—are of increasing interest [17–27].

Bismuth titanate of various compositions forms within the  $\text{TiO}_2$ – $\text{Bi}_2\text{O}_3$  phase diagram, including monoclinic  $\text{Bi}_2\text{Ti}_4\text{O}_{11}$ , sillenite-type  $\text{Bi}_{12}\text{TiO}_{20}$ , pyrochlore-type  $\text{Bi}_2\text{Ti}_2\text{O}_7$ , and the layered Aurivillius family compound  $\text{Bi}_4\text{Ti}_3\text{O}_{12}$ . Initially, scientific interest focused on the ferroelectric properties of bismuth titanate crystals for developing high-temperature sensors, memory devices, and transducers. Later, their photocatalytic properties attracted attention, for instance, for degrading dye pollutants and antibiotics from wastewater [19, 20]. According to Qin et al. [19], compounds based on the  $\text{TiO}_2$ – $\text{Bi}_2\text{O}_3$  system exhibit photocatalytic properties in the near-ultraviolet and visible spectral range because these compounds have a lower band energy gap ( $E_g$ ) than  $\text{TiO}_2$  ( $E_g = 3.2$  eV). Therefore, they may be more effective as photocatalysts (Table 1).

Table 1.  $E_g$  values for bismuth titanate compounds

Compound	$E_g$ value, eV
$\text{Bi}_2\text{Ti}_4\text{O}_{11}$	3.1
$\text{Bi}_{12}\text{TiO}_{20}$	2.9
$\text{Bi}_2\text{Ti}_2\text{O}_7$	2.5
$\text{Bi}_4\text{Ti}_3\text{O}_{12}$	2.95

Bismuth is often described as a “green,” eco-friendly metal capable of replacing lead and other heavy metals, thereby reducing their accumulation in the environment and mitigating heavy-metal pollution. Bismuth compounds are widely used in medicine for treating gastrointestinal diseases and as radiopaque agents, as well as in cosmetology, dental materials, and in industry for the production of lubricants and pigments [24]. It is also worth noting bismuth’s ability to inhibit the growth of mold, bacteria, and viruses due to its oligodynamic effect—the toxic impact of metal ions on living cells and microorganisms, even at relatively low trace concentrations [28]. Photocatalysts also suppress microbial growth, but through a different mechanism: their biocidal activity is explained by ROS formation and is usually limited in the dark [13].

Thus, in line with general trends in building materials science aimed at developing new multifunctional additives and modified building materials, and based on an analysis of scientific publications, the purpose of this work was defined as follows: to obtain a facade white cement-based composition modified with a multiphase  $\text{TiO}_2\text{--Bi}_2\text{O}_3$  additive, and to study its mechanical, photocatalytic, and biocidal properties. It is assumed that the additive based on bismuth titanates will impart self-cleaning properties to cement-based building materials through photocatalysis, as well as fungicidal activity not only through ROS formation under light exposure but also in the dark.

At the first stage of the study, the properties of the additive were analyzed using X-ray phase analysis and particle size distribution measurements, and its absorption range was determined. At the second stage, plaster compositions were prepared by dry mixing sand, white cement, plasticizer, and the additive in the required proportions, followed by mixing with tap water. The photocatalytic activity of the resulting samples and their resistance to mold growth were then evaluated according to standard test procedures. The next step involved measuring compressive and bending strength and testing adhesion to the substrate. Finally, the authors calculated the cost of the synthesized additive and the final product and identified the optimal composition for producing a self-cleaning, bio-resistant plaster. The research scheme is presented in Figure 2.

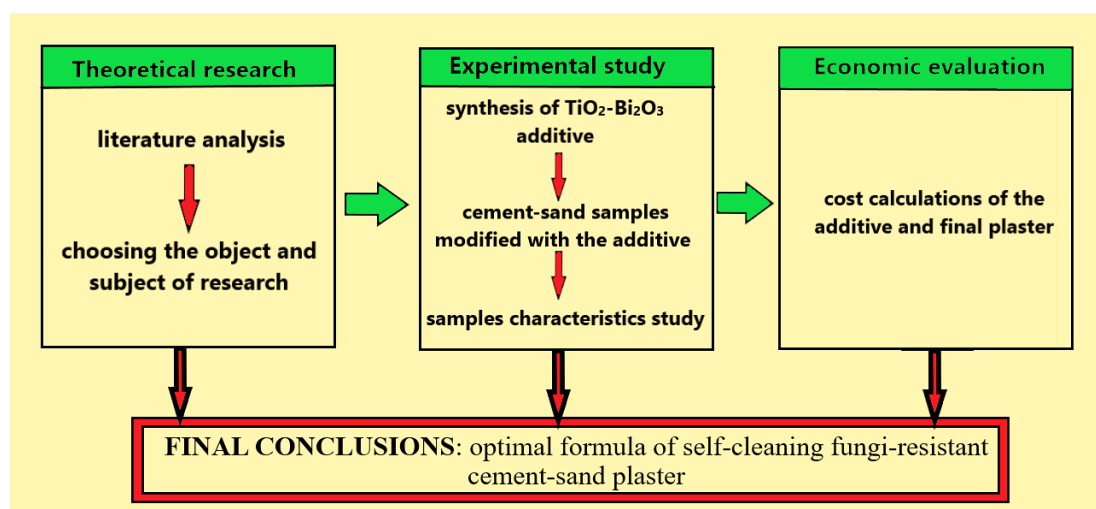
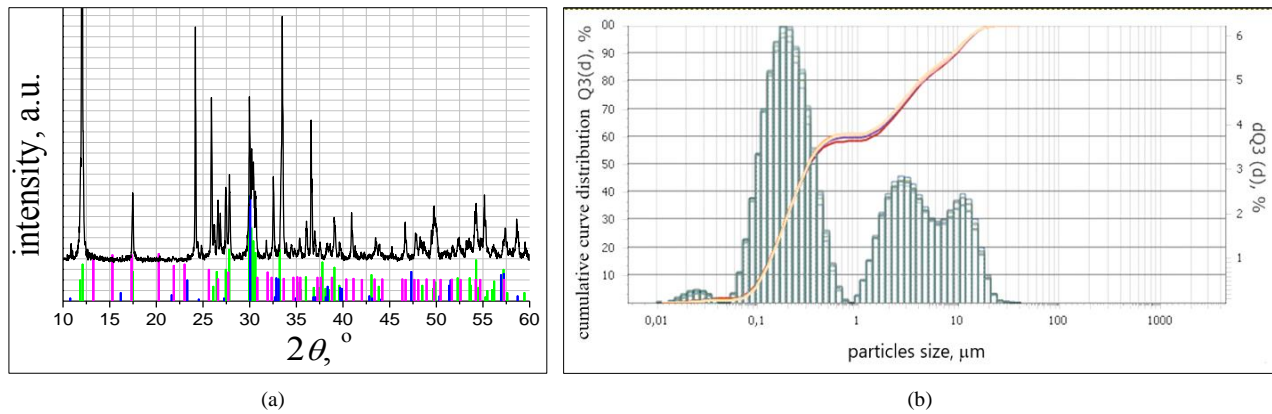


Figure 2. Schematic process of the research

## 2. Material and Methods

During this study, the authors used an additive obtained by citrate-based synthesis, with the detailed process described by Samchenko et al. [21] and Dhage et al. [29]. The synthesis of the additive was carried out according to the method described by Dhage et al. [29], using  $\text{TiCl}_4$  ( $\rho = 1.72 \text{ g/ml}$ ), analytical-grade  $\text{Bi}_2\text{O}_3$ , an HCl water solution (1:1), and citric acid monohydrate. The process was as follows:  $\text{TiCl}_4$  was dissolved in ice-cold distilled water under constant stirring to form Solution 1.  $\text{Bi}_2\text{O}_3$  was dissolved in HCl, after which citric acid was added to obtain Solution 2. Solutions 1 and 2 were then mixed, thoroughly stirred, and heated at  $100^\circ\text{C}$  to form a yellow dense gel, which was subsequently calcinated in a furnace at  $400^\circ\text{C}$  for 15 minutes and then at  $700^\circ\text{C}$  to obtain the final flake-like light-grey powder.

The phase composition of the bismuth titanate additive was studied using X-ray phase analysis (X-ray diffractometer D8 ADVANCE Bruker AXS,  $\text{CuK}\alpha$  radiation, graphite monochromator,  $\lambda_{\text{CuK}\alpha} = 1.54056 \text{ \AA}$ ). The X-ray diffraction patterns were processed using Match! software. According to the analysis, several phases were identified in the additive sample, with  $\text{Bi}_2\text{Ti}_4\text{O}_{11}$  (PDF#83-0673) being predominant, along with smaller amounts of layered  $\text{Bi}_4\text{Ti}_3\text{O}_{12}$  (PDF#72-1019) and  $\text{Bi}_2\text{Ti}_2\text{O}_7$  (PDF#32-0118) (Figure 3-a). Particle size analysis of the additive, conducted using the Analysette 22 NanoTec device (Fritsch, Germany), revealed several fractions of 0.33, 5, and 10 microns (Figure 3-b).



**Figure 3. (a) X-ray diffraction patterns of the additive: experimental data (black line);  $\text{Bi}_2\text{Ti}_4\text{O}_{11}$  (green line, PDF#83-0673);  $\text{Bi}_4\text{Ti}_3\text{O}_{12}$  (blue line, PDF#72-1019;  $\text{Bi}_2\text{Ti}_2\text{O}_7$  (pink line, PDF#32-0118)**

To determine the absorption range of the additive, a water-glycerin suspension of additive particles was prepared, and an SF-2000 spectrophotometer was used. Figure 4 shows the absorption spectra in the ultraviolet and visible spectra range at 250-800 nm wavelength.

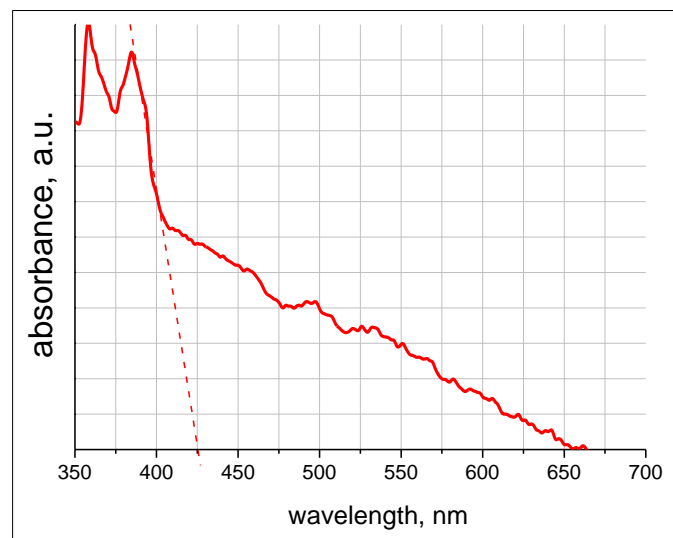


**Figure 4. UV-vis absorption spectrum of the synthesized additive**

In accordance with the study, the maximum absorption of the synthesized additive is 425 nm, which is the visible part of the spectra range. The band energy gap ( $E_g$ ) was calculated using the following equation:

$$E_g = \frac{hc}{\lambda} \quad (1)$$

where  $h$  is Planck constant,  $\lambda$  is the wavelength corresponding to the onset of absorbance, and  $c$  is the velocity of light. The calculated  $E_g$  value is 2.91 eV which indicates the additive photocatalytic ability in the visible spectra range.

The cement compositions were prepared by dry mixing of components (cement, sand and additive with plasticizer) in the required proportions, followed by mixing with tap water.

The materials used in the research:

- White Portland cement Cemix PRO WHITE 1-500 "Cemix Russia" Lasselsberger group GmbH, Pöchlarn, Austria (further mentioned as WPC). The clinker characteristics are presented in Tables 2 and 3;
- White quartz sand of 0.1- 0.4 mm fraction with the characteristics shown in Table 4.
- Polycarboxylate plasticizer Melflux 5581F (BASF Construction Additives, Germany).

**Table 2. Chemical composition of clinker LLC "Cemix PRO WHITE 1-500"**

Component	Calcination loss	CaO	SiO <sub>2</sub>	Al <sub>2</sub> O <sub>3</sub>	Fe <sub>2</sub> O <sub>3</sub>	MgO	SO <sub>3</sub>	R <sub>2</sub> O
%	1.0	65.0	21.0	5.5	0.5	1.0	3.3	0.1

**Table 3. Mineralogical composition of clinker LLC “Cemix PRO WHITE 1-500”**

Mineral content, %			
C <sub>3</sub> S	C <sub>2</sub> S	C <sub>3</sub> A	C <sub>4</sub> AF
66.0	8.5	13.5	1.5

**Table 4. Sand characteristics**

Bulk density g/cm <sup>3</sup>	Specific density, g/cm <sup>3</sup>	Grain size, μm	Oxide content, %							
			Clay	SiO <sub>2</sub>	Al <sub>2</sub> O <sub>3</sub>	Fe <sub>2</sub> O <sub>3</sub>	CaO	MgO	K <sub>2</sub> O	TiO <sub>2</sub>
1.403	2.64	235.23	0.10	99.86	0.130	0.026	-	0.003	0.021	0.018

The photocatalytic activity of the obtained samples was studied in accordance with the Italian standard UNI 11259-2016 [30], which consists of fixing the discoloration (mineralization) of the organic pigment Rhodamine B applied to the surface of the sample modified with a photocatalyst when exposed to UV radiation after 4 and 26 hours.

The photocatalytic activity of the samples was estimated by changing parameter  $a$  and calculated using the following formulas:

$$R_4 = \frac{a_0 - a_4}{a_0} \cdot 100\% \quad (2)$$

$$R_{26} = \frac{a_0 - a_{26}}{a_0} \cdot 100\% \quad (3)$$

where  $a_0$  is the value of the color coordinate at initial time;  $a_4$  is the value of the color coordinate after 4 hours of radiation;  $a_{26}$  is the value of the color coordinate after 26 hours of radiation. The  $R$  values should be more than 20% after 4 hours and more than 50% after 26 hours of exposure, according to the UNI 11259 standard.

Samples for testing resistance to mold fungi were 30×30 mm cubes, including control and modified samples. The test procedure was carried out at the A.N. Severtsov Institute of Ecology and Evolution of the Russian Academy of Sciences (IEE RAS) in the laboratory of tropical technologies in accordance with the Standard 9.048-89 [31]. The surface of the samples was contaminated with a suspension of *Aspergillus niger* van Tieghem, *Aspergillus terreus* Thom, *Aureobasidium pullulans* (de Bary) Arnaud, *Paecilomyces varioti* Bainier, *Penicillium funiculosum* Thom, *Penicillium ochro-chloron* Biourge, *Scopulariopsis brevicaulis* Bainier, *Trichoderma viride* Pers. Ex Fr. spores with concentration of 1-2 million/cm<sup>3</sup>. Contaminated samples were held at conditions optimal for growth and sporulation of fungi at 27-28°C and 98% humidity for 28 days. Fungi cultures are supplied at sealed tubes and restored. The recovered cultures are transferred into tubes with agar nutrient medium. One part is left stored; the other is the initial one for obtaining working batches of fungi cultures. Fungi suspension is made from a culture grown for two weeks. At the end of the test, the stage of fungi development was evaluated on a 6-point scale:

"0" points – absolutely clean samples, growth of mycelium and conidia was not detected visually and under a microscope;

"1" point – sprouted spores and a slightly developed mycelium are visible under the microscope;

"2" points – the developed mycelium is visible under the microscope in the form of numerous spots on the surface of the sample, absence of sporulation;

"3" points – intense growth of the mycelium on the surface of the sample, beginning of sporulation;

"4" points – the entire mycelium growth and sporulation are clearly visible;

"5" points – deep mycelium growth, the entire surface of the sample is damaged, intensive sporulation is observed.

The mechanical tests were conducted in accordance with Russian Standard P 58277—2018 [32]. For flexural strength determination, control and modified with the additive prism samples of 40×40×160 mm was obtained. The compressive strength was determined by testing six halves of the prism samples obtained during the flexural strength test. Strength tests were conducted using a laboratory hydraulic press (Controls 50-C8455, Italy).

For the adhesion to substrate test [32] 10 mm thick plaster samples were prepared by filling the 50×50 square mold, placed on a concrete base. During the period of structure formation (before the beginning of hardening), conical rings are pressed into the mixture layer, rotating, to the base. Then, continuing the rotation, the rings are carefully removed. The samples are stored for 7 days at a temperature of  $20 \pm 2^\circ\text{C}$  and relative humidity  $(95 \pm 5)\%$  before the test, and then for 21 days at a temperature of  $(20 \pm 2)^\circ\text{C}$  and relative humidity  $(60 \pm 10)\%$ . The test was conducted at 28 days age. After 27 days, a stamp is glued to the hardened samples with epoxy or other fast-hardening adhesive of high strength

and the samples are stored at a temperature of  $(20 \pm 2)^{\circ}\text{C}$  and relative humidity  $(60 \pm 10)\%$  for 24 hours. The separation force of the samples from the base is determined after 24 hours. The adhesion test was conducted using digital adhesion tester DeFelsko PosiTest AT-M (USA).

### 3. Results

For the research a dry mixture of sand and WPC was prepared at 3.5:1 weight ratio, then the mixture of the additive (at 1.7 and 5.0 wt.%) with the plasticizer (0,12 wt.%) was added. Water-to-cement ratio was 0.85 for all samples, determined in accordance with mortar workability.

The prepared mortars, including reference and modified ones, were studied for mold fouling resistance at 28 days age at the A.N. Severtsov Institute of Ecology and Evolution of the Russian Academy of Sciences (IEE RAS) in the laboratory of tropical technologies. The results of the study are shown at Table 5 and Figure 5. The test shows that modified samples are resistant to fouling, the fouling assessment is 0 points.

**Table 5. Assessment of the fungi resistance of cement plaster samples**

Sample	Visual shape after the test	Evaluation of Biostability, points	Additive content, %	Biostability, %
1-1 Control	Mycelium growth on the surface of the sample, the beginning of sporulation	3	0	30
1-2 Control	Mycelium growth on the surface of the sample, the beginning of sporulation	3	0	30
1-3 Control	Mycelium growth and sporulation are clearly visible	4	0	20
2-1	Spore growth, conidia and colony development is not observed under the microscope	0	1,7	100
2-2	Spore growth, conidia and colony development is not observed under the microscope	0	1,7	100
2-3	Spore growth, conidia and colony development is not observed under the microscope	0	1,7	100
3-1	Spore growth, conidia and colony development is not observed under the microscope	0	5,0	100
3-2	Spore growth, conidia and colony development is not observed under the microscope	0	5,0	100
3-3	Spore growth, conidia and colony development is not observed under the microscope	0	5,0	100

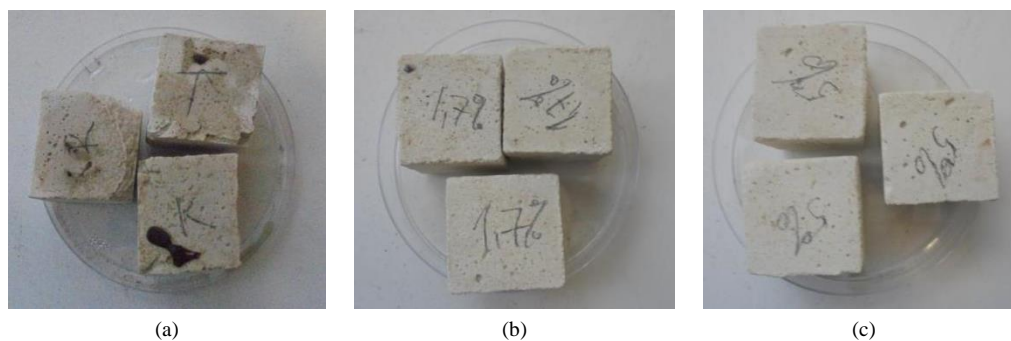


**Figure 5. Samples of cement plaster composition: (a) control; (b) with 1.7 wt.% of the additive; (c) with 5 wt.% of the additive after 28 days of testing in the thermostat**

Spore growth, conidia, and colony development were not detected under the microscope. Samples No. 2-1, 2-2, 2-3, 3-1, 3-2, 3-3 are 100%-fungi resistant according to the test procedure assessment. The control samples were subjected to biofouling with an assessment of 3-4 points; biostability is 20-30%. According to the microscopic investigation, the color, shape, and structure of the mycelium on the surface of the control samples allowed the authors to determine mainly the presence of *Aspergillus niger*, *Aspergillus terreus*, and *Scopulariopsis brevicaulis*. Based on the test data, it can be concluded that compositions modified with an additive in amounts of 1.7 wt.% and more are resistant to biofouling. Thus, it has been experimentally confirmed that the production of a cement composition modified with an additive based on  $\text{TiO}_2 - \text{Bi}_2\text{O}_3$  is resistant to fouling with microscopic mold fungi, while the amount of the additive sufficient for the biocidal properties of the building material is 1.7 wt.%.

For comparison, previous studies [33–35] have reported the fungicidal activity of various nanoscale photocatalysts, including  $\text{TiO}_2$  and  $\text{ZnO}$  metal oxides in both pure form and doped with Ag, Au, Ni, and Cu. However, this activity is performed at relatively high light intensity and explained by the influence of ROS formed on the surface of a semiconductor photocatalyst. Whereas in the dark, their fungicidal activity is insignificant or has not been studied.

In studies [24, 36–38], the photocatalytic, fungicidal, and antimicrobial properties of  $\text{BiVO}_4$  and  $\text{BiOCl}$  compounds, in both pure and doped forms, have also been investigated. And while the photocatalytic oxidation of organic pigments due to the formation of ROS has been studied in detail in the literature, the effect on mold fungi, bacteria, and viruses



remains poorly understood. According to Mosquera-Sánchez et al. [39] and Saikia et al. [40], zinc salts are harmful to mold fungi due to the fact that they slow down the production of chitin by fungal cells, which is the main component of cell walls. Copper-based fungicides are widespread; however, their accumulation in soils and waters is a serious problem for human health and the environment [41, 42].

Therefore, according to the literature data, there are three main approaches explaining the effect of nanostructured photocatalysts on the growth and development of microscopic mold fungi. The first is the destructive action of ROS formed under the influence of light. The second is explained by the size and morphology of the additive particles. A special type of interaction between nanoparticles and cell membranes occurs, which disrupts their life cycle and metabolic processes inside a cell, leading to its death. The third is oligodynamic action, a biocidal effect of metals, especially heavy metals (Zn, U, Ag, Au), that occurs even in low concentrations and leads to microorganism cell death [43, 44]. Thus, it can be concluded that a multiphase additive based on bismuth titanates exhibits fungicidal activity due to these three factors, both in the light and in the dark (Figure 6).

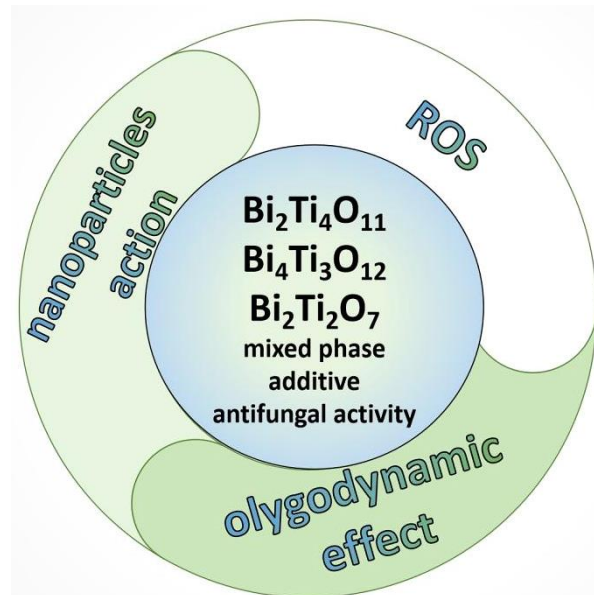


Figure 6. Factors that ensure the fungicidal activity of the additive

The photocatalytic activity of the cement mortars was evaluated in accordance with the Italian standard UNI 11259-201. For the test square plates of 5.0×5.0 cm and 1 cm thickness were prepared. As a result of the study of the photocatalytic activity of modified samples of self-cleaning cement composition, the following results were obtained, shown in Figures 7 and 8.

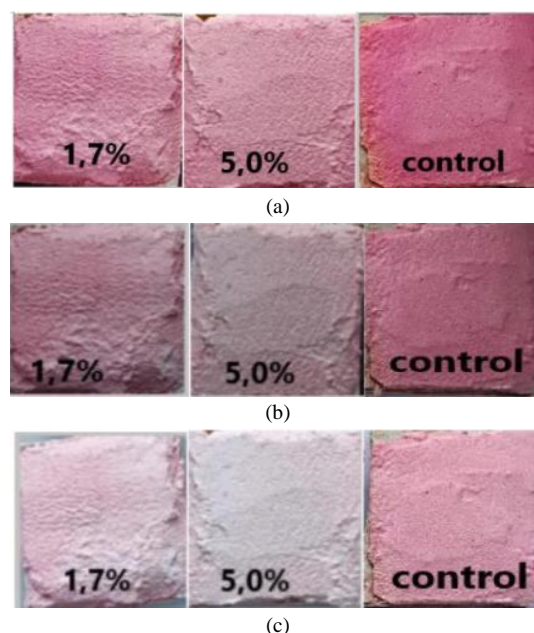
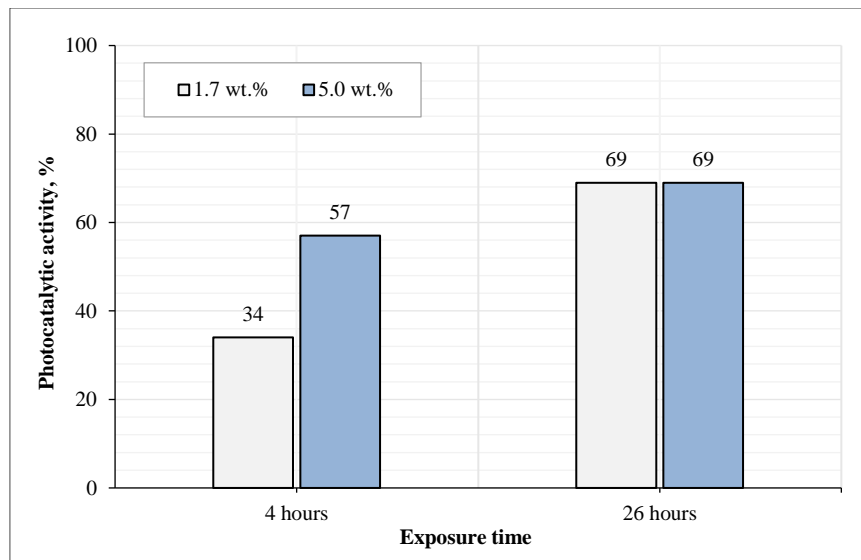


Figure 7. Discoloration of Rhodamine B after UV exposure of the samples with  $\text{TiO}_2$  -  $\text{Bi}_2\text{O}_3$  additive (a) at before irradiation (b) after 4 hours (c) after 26 hours of UV irradiation



**Figure 8. Photocatalytic activity of cement plaster samples modified with  $\text{TiO}_2 - \text{Bi}_2\text{O}_3$  additive**

From the data presented in Figure 7, it can be concluded that the samples with the synthesized additive demonstrate photocatalytic activity both after 4 hours and after 26 hours of UV exposure. The maximum photocatalytic activity (57 - 69%) is achieved for samples with  $\text{TiO}_2\text{-Bi}_2\text{O}_3$  additive in amount of 5.0 wt.%. Samchenko et al. [21] conducted by the authors on samples of pure white cement with an additive indicate that the photocatalytic parameters correspond to the sample, starting with 5% of the additive. This can be explained by the addition of sand because it makes the surface of the sample rough with higher specific surface area than the smooth one. Therefore, a large number of active centers are involved in photocatalytic oxidation reactions. On the other hand, a more textured surface of the material will be more easily contaminated by oxidation products and dust particles from the air, which requires further study [45].

The strength properties of the modified compounds were also tested:

- Composition with 1.7 wt.% of the additive;
- Composition with 5 wt.% of the additive.

The total data of the samples' tests are combined in the Table 6

**Table 6. Properties of cement compositions**

Characteristic	Unit	Value		
		Control	Composition 1	Composition 2
Compressive strength	MPa	39.8	52.4	55.3
Flexural strength	MPa	5.5	7.3	7.6
Adhesion to Substrate	MPa	0.5	0.8	0.85
Photocatalytic activity after 26 h	%	0	69	69
Fungi growth	point	3	0	0
Biostability	-	Non-resistant to fungi	Fungi-resistant	Fungi-resistant

The results of the study showed that the modified compositions are both photocatalytically active and fungi-resistant and also have increased mechanical properties: the compressive strength of the modified compositions increased by 32.0-39.0% from 39.8 to 52.4-55.3 MPa; flexural strength—by 33-38.0% from 5.5 to 7.3-7.6 MPa; and adhesion—by 60-70% from 0.5 to 0.8-0.85 MPa.

According to previous studies [46, 47], the incorporation of fine particles and nanoparticles into cement enhances its physical and mechanical properties. Nanoscale particles of semiconductor photocatalysts do not possess their own hydraulic activity, but they can act as crystallization centers, promoting the formation and growth of hydration products in cement grains. It is important that the additive particles be uniformly distributed in the cement paste—this can be achieved by adding a plasticizer, applying ultrasonication, or using both methods [48, 49]. In such cases, the photocatalyst additive positively influences the hydration process of cement clinker minerals and improves the mechanical properties of mortar and cement stone.



In a previous study, the authors investigated the effect of the additive on ordinary Portland cement (OPC). Kozlova & Dudareva [48] and Jiang et al. [49] discuss different methods for introducing the fine additive based on the  $\text{TiO}_2 - \text{Bi}_2\text{O}_3$  system into cement compositions. The article examines samples obtained by:

1. dry mixing of cement and the additive with tap water,
2. cement + additive suspension after ultrasonic treatment,
3. cement + additive + water–plasticizer solution,
4. cement + additive water–polymer suspension stabilized by ultrasonication.

The compressive strength of the samples was evaluated, and the highest strength was recorded for the sample containing 1.7 wt.% of the additive: an increase of 44.8% at one day of age and 14.0% at 28 days compared to the control sample containing cement, water, and plasticizer. This sample also showed a reduction in porosity due to the filling effect. These data confirm that the additive exhibits a structure-forming effect when introduced into OPC, as well as into white cement.

The results of the study show that introducing the additive into the plaster composition contributes to the creation of a self-cleaning, fungi-resistant building material with improved strength characteristics. The findings also indicate that adding the additive at 5 wt.% does not significantly enhance the properties of the resulting material: the modified Composition 1 exhibits nearly the same improved characteristics as Composition 2. Therefore, to obtain a fungi-resistant cement plaster composition with photocatalytic self-cleaning capability, it is sufficient to introduce the additive in an amount of 1.7 wt.% of the dry mixture.

#### 4. Discussion

As a result of the study, the authors obtained polyfunctional  $\text{TiO}_2 - \text{Bi}_2\text{O}_3$  additive for cement systems synthesized via citrate-based technology, which includes phases  $\text{Bi}_2\text{Ti}_4\text{O}_{11}$  (PDF#83-0673), perovskite-like  $\text{Bi}_4\text{Ti}_3\text{O}_{12}$  (PDF#72-1019) and a metastable  $\text{Bi}_2\text{Ti}_2\text{O}_7$  (PDF#32-0118) with particle size of 0.33, 5 and 10  $\mu\text{m}$ . The introduction of the additive into the cement composition allows to design bio-stable materials with photocatalytic effect and enhanced mechanical characteristics. The approximate composition of self-cleaning cement material is shown in Table 7.

**Table 7. Approximate composition of self-cleaning composition**

WPC 1-500, kg	Sand, kg	$\text{TiO}_2 - \text{Bi}_2\text{O}_3$ additive (5 wt.%), kg	Plasticizer (0.12 wt.%), kg	WPC 1-500, kg
1	150	525	11.475	0.81
2	150	525	33.750	0.81

Tables 8 and 9 present the cost calculation of the of the additive for Compositions 1 and 2, respectively

**Table 8. Amount and cost of materials for the production of synthesized additive for Composition 1**

Material	Units	Amount for the production of 11.475 kg additive	Price, USD	Cost, USD
$\text{Bi}_2\text{O}_3$	kg	6.31	46.3	292.15
$\text{TiCl}_4$	l	5.74	23.15	132.88
Citric acid	kg	25.82	4.17	107.67
HCl	l	14.34	2.52	36.14
Distilled water	l	14.34	1.81	25.96
Energy	kW·h	332.76	0.048	15.97
<b>Total</b>				<b>610.77</b>

**Table 9. Amount and cost of materials for the production of synthesized additive for Composition 2**

Material	Units	Amount for the production of 11.475 kg additive	Price, USD	Cost, USD
$\text{Bi}_2\text{O}_3$	kg	18.56	46.3	859.33
$\text{TiCl}_4$	l	16.88	23.15	390.77
Citric acid	kg	75.94	4.17	316.67
HCl	l	42.18	2.52	106.29
Distilled water	l	42.18	1.81	76.35
Energy	kW·h	978.71	0.048	46.98
<b>Total</b>				<b>1796.39</b>

The calculation of the cost of the synthesized additive for obtaining a modified Composition 1 with 1.7 wt.% of the additive was 610.77 USD; for Composition 2 with 5.0 wt.% of the additive, it was 1796.39 USD, which is 3 times higher than for the production of Composition 1. Tables 10 and 11 present the calculation of the cost of self-cleaning plasters for Compositions 1 and 2, respectively.

**Table 10. Amount and cost of materials for the production of self-cleaning Composition 1**

Material	Units	Amount, kg	Price, USD	Cost, USD
WPC 1-500 D0	ton	0.15	190.74	28.61
Sand (average grain size 0.2 mm)	ton	0.525	166.67	87.50
Additive	kg	11.475	53.23	610.77
Plasticizer	kg	0.81	3.66	2.96
<b>Total</b>				<b>729.84</b>

**Table 11. Amount and cost of materials for the production of self-cleaning Composition 2**

Material	Units	Amount, kg	Price, USD	Cost, USD
WPC 1-500 D0	ton	0.15	190.74	28.61
Sand (average grain size 0.2 mm)	ton	0.525	166.67	87.50
Additive	kg	33.75	53.23	1796.39
Plasticizer	kg	0.81	3.66	2.96
<b>Total</b>				<b>1915.46</b>

The calculation of the cost of self-cleaning Composition 1 is 729.84 USD, while for Composition 2 it is 1915.46 USD, which is 2.6 times higher than that of plaster Composition 1. The calculations showed that introducing the synthesized additive into the cement–sand mixture at 5.0 wt.% is not advisable, since the photocatalytic and mechanical characteristics only slightly exceed those of the composition with 1.7 wt.% additive, while the cost of Composition 2 increases almost threefold.

The analysis showed that Composition 1 presented in Table 10 can be used as a basis for designing recommendations for self-cleaning, bio-resistant dry mixture production. Thus, it is proposed to use a WPC:sand ratio (average grain size 0.2 mm) of 1:3.5 and W/C = 0.85. The additive based on the  $\text{TiO}_2\text{--Bi}_2\text{O}_3$  oxide system at 1.7 wt.% is mixed with a polycarboxylate plasticizer at 0.12 wt.%. The mixture of additive and plasticizer is introduced into the previously prepared cement–sand mixture and mixed in any mixer until a homogeneous state is achieved. The quantities of materials for designing the self-cleaning plaster in Table 10 are approximate and should be refined considering the properties of the starting materials.

## 5. Conclusion

In this study, a technology for producing self-cleaning, bio-stable cement compositions modified with a  $\text{TiO}_2\text{--Bi}_2\text{O}_3$  additive synthesized via a citrate-based method was developed. According to the characterization of the additive, its granulometric composition consists of three main fractions—0.33, 5, and 10 microns—and its maximum absorption is at 425 nm, which lies in the visible part of the spectrum. This enables more efficient utilization of natural solar irradiation in photocatalytic oxidation processes. The additive was then introduced into a cement–sand mixture to obtain plaster samples, and their resistance to fungi, photocatalytic activity, and mechanical properties were investigated.

The tests showed that samples containing the additive at 1.7 wt.% and above were resistant to *Aspergillus niger* van Tieghem, *Aspergillus terreus* Thom, *Aureobasidium pullulans* (de Bary) Arnaud, *Paecilomyces varioti* Bainier, *Penicillium funiculosum* Thom, *Penicillium ochro-chloron* Biourge, *Scopulariopsis brevicaulis* Bainier, and *Trichoderma viride* Pers. Ex Fr.

The photocatalytic activity of the samples after 4 hours of irradiation ranged from 34–57%, and after 26 hours reached 69%. The tests also showed increased mechanical performance of the modified samples: compressive strength increased by 32.0–39.0% (from 39.8 MPa to 52.4–55.3 MPa); flexural strength increased by 33–38.0% (from 5.5 MPa to 7.3–7.6 MPa); and adhesion strength increased by 60–70% (from 0.5 MPa to 0.8–0.85 MPa). The results demonstrated that samples with 1.7 wt.% of the synthesized additive achieved nearly the same enhanced properties as those with 5.0 wt.% additive. The cost analysis further confirmed the feasibility of introducing the  $\text{TiO}_2\text{--Bi}_2\text{O}_3$  additive at 1.7 wt.% into the cement composition, costing 729 USD—almost three times less than a composition containing 5.0 wt.% of the additive. The final cement formulation can therefore be recommended for designing fungi-resistant, self-cleaning plasters.

## 6. Declarations

### 6.1. Author Contributions

Conceptualization, I.K., S.S., and O.Z.; methodology, S.S. and A.K.; validation, S.S. and O.Z.; formal analysis, I.K., S.S., and O.Z.; investigation, S.S., O.Z., and M.D.; resources, I.K., S.S., and O.Z.; data processing, S.S., O.Z., and M.D.; writing—original draft preparation, M.D.; writing—review and editing, S.S., I.K., and O.Z.; visualization, I.K., S.S., and O.Z.; supervision, S.S. and A.K.; project administration, I.K., S.S., and M.D.; funding acquisition, S.S. and A.K. All authors have read and agreed to the published version of the manuscript.

### 6.2. Data Availability Statement

The data presented in this study are available in the article.

### 6.3. Funding

The research was funded by the National Research Moscow State University of Civil Engineering (grant for fundamental scientific research, project No. 10-661/130).

### 6.4. Acknowledgements

This research was carried out using the facilities of the Head Regional Shared Research Facilities of the Moscow State University of Civil Engineering, with support from the Ministry of Science and Higher Education of the Russian Federation (Agreement No. 075-15-2025-549).

### 6.5. Conflicts of Interest

The authors declare no conflict of interest.

## 7. References

- [1] Pilipenko, A., Bobrova, E., & Zhukov, A. (2019). Optimization of plastic foam composition for insulation systems. *E3S Web of Conferences*, 91. doi:10.1051/e3sconf/20199102017.
- [2] Novikov, N. V., Samchenko, S. V., & Okolnikova, G. E. (2020). Barite-containing radiation protective building materials. *RUDN Journal of Engineering Researches*, 21(1), 94–98. doi:10.22363/2312-8143-2020-21-1-94-98.
- [3] Ali, M. A. E. M., Hafez, M. A. Y., Nagy, N. M., & Abed, N. S. (2025). Radiation shielding properties of sustainable concrete with novel plastering techniques. *Annals of Nuclear Energy*, 211. doi:10.1016/j.anucene.2024.110958.
- [4] Hegyi, A., Grebenişan, E., Lăzărescu, A. V., Stoian, V., & Szilagyi, H. (2021). Influence of TiO<sub>2</sub> nanoparticles on the resistance of cementitious composite materials to the action of fungal species. *Materials*, 14(16), 1–18. doi:10.3390/ma14164442.
- [5] Ubaldi, F., Valeriani, F., Volpini, V., Lofrano, G., & Romano Spica, V. (2024). Antimicrobial Activity of Photocatalytic Coatings on Surfaces: A Systematic Review and Meta-Analysis. *Coatings*, 14(1), 1–30. doi:10.3390/coatings14010092.
- [6] Strokova, V., Ogurtsova, Y., Gubareva, E., Nerovnaya, S., & Antonenko, M. (2024). Multifunctional Anatase–Silica Photocatalytic Material for Cements and Concretes. *Journal of Composites Science*, 8(6), 1–19. doi:10.3390/jcs8060207.
- [7] Balykov, A., Nizina, T., & Volodin, S. (2023). Technological efficiency of mineral modifiers for cement materials with photocatalytic activity. *E3S Web of Conferences*, 458(5), 1–6. doi:10.1051/e3sconf/202345802026.
- [8] Alshabander, B., & Abd-alkader, M., B. (2023). Photocatalytic Degradation of Methyl blue by TiO<sub>2</sub> Nanoparticles Incorporated in Cement. *Iraqi Journal of Physics*, 21(1), 10–20. doi:10.30723/ijp.v20i1.1042.
- [9] Lapidus, A., Korolev, E., Topchiy, D., Kuzmina, T., Shekhovtsova, S., & Shestakov, N. (2022). Self-Cleaning Cement-Based Building Materials. *Buildings*, 12(5), 1–24. doi:10.3390/buildings12050606.
- [10] Khannyra, S., Mosquera, M. J., Addou, M., & Gil, M. L. A. (2021). Cu-TiO<sub>2</sub>/SiO<sub>2</sub> photocatalysts for concrete-based building materials: Self-cleaning and air de-pollution performance. *Construction and Building Materials*, 313, 1–15. doi:10.1016/j.conbuildmat.2021.125419.
- [11] Truppi, A., Luna, M., Petronella, F., Falcicchio, A., Giannini, C., Comparelli, R., & Mosquera, M. J. (2018). Photocatalytic activity of TiO<sub>2</sub>/AuNRs-SiO<sub>2</sub> nanocomposites applied to building materials. *Coatings*, 8(9), 1–20. doi:10.3390/COATINGS8090296.
- [12] Putri, J. E. Y., & Pratama, M. M. A. (2023). Photocatalytic Concrete Using ZnO and Al<sub>2</sub>O<sub>3</sub> - A Review. *E3S Web of Conferences*, 445, 1–7. doi:10.1051/e3sconf/202344501028.

- [13] Al Hallak, M., Verdier, T., Bertron, A., Castelló Lux, K., El Atti, O., Fajerweg, K., Fau, P., Hot, J., Roques, C., & Bailly, J. D. (2023). Comparison of Photocatalytic Biocidal Activity of TiO<sub>2</sub>, ZnO and Au/ZnO on *Escherichia coli* and on *Aspergillus niger* under Light Intensity Close to Real-Life Conditions. *Catalysts*, 13(7), 1–15. doi:10.3390/catal13071139.
- [14] Sharafutdinov, K. B., Saraykina, K. A., Kashevarova, G. G., & Erofeev, V. T. (2022). the Use of Copper Nanomodified Calcium Carbonate as a Bactericidal Additive for Concrete. *International Journal for Computational Civil and Structural Engineering*, 18(2), 143–155. doi:10.22337/2587-9618-2022-18-2-143-155.
- [15] Latyshevich, I. A., Hapankova, A. I., Kozlov, N. G., & Hliavitskaya, T. A. (2024). Biocide Additives (Review). *Bulletin of the Saint Petersburg State Institute of Technology (Technical University)*, 69, 59–68. doi:10.36807/1998-9849-2024-69-95-59-68.
- [16] Erofeev, V.T., Rodin, A.I., Karpushin, S.N., Sanyagina, Y.A., Klyuev, S.V., Sabitov, L.S. (2023). Biological and Climatic Resistance of Cement Composites Based on Biocidal Binders. *Innovations and Technologies in Construction. BUILDINTECH BIT 2022. Lecture Notes in Civil Engineering*, vol 307. Springer, Cham, Switzerland. doi:10.1007/978-3-031-20459-3\_22.
- [17] Liu, X., Xu, H., Li, D., Zou, Z., & Xia, D. (2019). Facile Preparation of BiOCl/ZnO Heterostructure with Oxygen-Rich Vacancies and Its Enhanced Photocatalytic Performance. *ChemistrySelect*, 4(42), 12245–12251. doi:10.1002/slct.201902964.
- [18] Teng, D., Qu, J., Li, P., Jin, P., Zhang, J., Zhang, Y., & Cao, Y. (2022). Heterostructured  $\alpha$ -Bi<sub>2</sub>O<sub>3</sub>/BiOCl Nanosheet for Photocatalytic Applications. *Nanomaterials*, 12(20), 1–14. doi:10.3390/nano12203631.
- [19] Qin, K., Zhao, Q., Yu, H., Xia, X., Li, J., He, S., Wei, L., & An, T. (2021). A review of bismuth-based photocatalysts for antibiotic degradation: Insight into the photocatalytic degradation performance, pathways and relevant mechanisms. *Environmental Research*, 199, 1–13. doi:10.1016/j.envres.2021.111360.
- [20] Wang, J., Liu, W., Zhong, D., Ma, Y., Ma, Q., Wang, Z., & Pan, J. (2019). Fabrication of bismuth titanate nanosheets with tunable crystal facets for photocatalytic degradation of antibiotic. *Journal of Materials Science*, 54(21), 13740–13752. doi:10.1007/s10853-019-03882-1.
- [21] Samchenko, S. V., Kozlova, I. V., Korshunov, A. V., Zemskova, O. V., & Dudareva, M. O. (2023). Synthesis and Evaluation of Properties of an Additive Based on Bismuth Titanates for Cement Systems. *Materials*, 16(18), 1–13. doi:10.3390/ma16186262.
- [22] Jia, J., Wang, Q., & Wang, Y. (2019). Synthesis of Bi<sub>2</sub>TiO<sub>5</sub>/TiO<sub>2</sub> heterojunction with enhanced visible-light photocatalytic activity and mechanism insight. *Journal of Alloys and Compounds*, 809, 1–9. doi:10.1016/j.jallcom.2019.151791.
- [23] Vazquez-Munoz, R., Lopez, F. D., & Lopez-Ribot, J. L. (2020). Bismuth nanoantibiotics display anticandidal activity and disrupt the biofilm and cell morphology of the emergent pathogenic yeast *Candida auris*. *Antibiotics*, 9(8), 1–15. doi:10.3390/antibiotics9080461.
- [24] Rosário, J. dos S., Moreira, F. H., Rosa, L. H. F., Guerra, W., & Silva-Caldeira, P. P. (2023). Biological Activities of Bismuth Compounds: An Overview of the New Findings and the Old Challenges Not Yet Overcome. *Molecules*, 28(15), 1–30. doi:10.3390/molecules28155921.
- [25] Palanisamy, K., Gurunathan, V., & Sivapriya, J. (2023). Biogenic Synthesis of Bismuth Oxide Nanoparticles and Its Antifungal Activity. *Oriental Journal of Chemistry*, 39(3), 608–613. doi:10.13005/ojc/390310.
- [26] Noviyanti, A. R., Eddy, D. R., Permana, M. D., & Risdiana. (2023). Heterophase of Bismuth Titanate as a Photocatalyst for Rhodamine B Degradation. *Trends in Sciences*, 20(10), 1–10. doi:10.48048/tis.2023.6147.
- [27] Chen, K., Scott, J., Qu, F., Dong, W., Tsang, D. C., & Li, W. (2025). Advanced cement-based photocatalytic materials: Strategies for agglomeration control, aging resistance and process optimisation. *Journal of Building Engineering*, 113816. doi:10.1016/j.jobbe.2025.113816.
- [28] Mittapally, S., Taranum, R., & Parveen, S. (2018). Metal ions as antibacterial agents. *Journal of Drug Delivery and Therapeutics*, 8(6-s), 411–419. doi:10.22270/jddt.v8i6-s.2063.
- [29] Dhage, S. R., Kholam, Y. B., Dhespande, S. B., Potdar, H. S., & Ravi, V. (2004). Synthesis of bismuth titanate by citrate method. *Materials Research Bulletin*, 39(13), 1993–1998. doi:10.1016/j.materresbull.2004.07.014.
- [30] UNI EN 11259:2016. (2016). Determination of the Photocatalytic Activity of Hydraulic Binders-Rodammina Test Method. UNI Ente Nazionale Italiano di Unificazione, Milano, Italy.
- [31] GOST 9.048-89. (1989). Unified system of corrosion and ageing protection. Technical items. Methods of laboratory tests for mould resistance. USSR Standardization Institute, Moscow, Russia. (In Russian).
- [32] GOST R 58277. (2018). Dry building mixes on cement binder. Test methods. USSR Standardization Institute, Moscow, Russia. (In Russian).
- [33] Whitehead, K. A., Brown, M., Caballero, L., Lynch, S., Edge, M., Hill, C., Verran, J., & Allen, N. S. (2025). Nano-Titania Photocatalysis and Metal Doping to Deter Fungal Growth on Outdoor and Indoor Paint Surfaces Using UV and Fluorescent Light. *Micro*, 5(1), 5. doi:10.3390/micro5010005.

- [34] Chi, M., Gu, L., Liu, K., Lin, J., Wang, Q., Yu, B., Wang, Z., Fu, X., Li, D., Zhao, G., & Li, C. (2025). The effect and mechanism of enhanced photocatalytic fungicidal activity on nitrogen doped carbon dots-modified titanium dioxide. *Carbon*, 238, 120314. doi:10.1016/j.carbon.2025.120314.
- [35] Hernandez, R., Jimenez-Chávez, A., De Vizcaya, A., Lozano-Alvarez, J. A., Esquivel, K., & Medina-Ramírez, I. E. (2023). Synthesis of TiO<sub>2</sub>-Cu<sup>2+</sup>/CuI Nanocomposites and Evaluation of Antifungal and Cytotoxic Activity. *Nanomaterials*, 13(13), 1900. doi:10.3390/nano13131900.
- [36] Pramila, S., Mallikarjunaswamy, C., Lakshmi Ranganatha, Nagaraju, G., Kavana, C. P., Chandan, S., & Spoorthy, H. P. (2024). Green synthesis of bismuth vanadate nanostructures for efficient photocatalytic and biological studies. *Nano-Structures & Nano-Objects*, 39, 101198. doi:10.1016/j.nanoso.2024.101198.
- [37] Mallikarjunaswamy, C., Pramila, S., Shivaganga, G. S., Deepakumari, H. N., Prakruthi, R., Nagaraju, G., Parameswara, P., & Lakshmi Ranganatha, V. (2023). Facile synthesis of multifunctional bismuth oxychloride nanoparticles for photocatalysis and antimicrobial test. *Materials Science and Engineering: B*, 290, 1–9. doi:10.1016/j.mseb.2023.116323.
- [38] Theodorakopoulos, G. V., Pylarinou, M., Sakellis, E., Katsaros, F. K., Likodimos, V., & Romanos, G. E. (2024). Mo-BiVO<sub>4</sub> Photocatalytically Modified Ceramic Ultrafiltration Membranes for Enhanced Water Treatment Efficiency. *Membranes*, 14(5), 1–16. doi:10.3390/membranes14050112.
- [39] Mosquera-Sánchez, L. P., Arciniegas-Grijalba, P. A., Patiño-Portela, M. C., Guerra-Sierra, B. E., Muñoz-Florez, J. E., & Rodríguez-Páez, J. E. (2020). Antifungal effect of zinc oxide nanoparticles (ZnO-NPs) on *Colletotrichum* sp., causal agent of anthracnose in coffee crops. *Biocatalysis and Agricultural Biotechnology*, 25, 101579. doi:10.1016/j.bcab.2020.101579.
- [40] Saikia, R., Sharma, S., Kaman, P., & Chatterjee, A. (2025). Antifungal Efficacy of Green-Synthesized Zinc Oxide Nanoparticles Against *Fusarium* Spp.: an in Vitro Study. *Plant Archives*, 25(1), 1027–1036. doi:10.51470/plantarchives.2025.v25.no.1.154.
- [41] Parada, J., Tortella, G., Seabra, A. B., Fincheira, P., & Rubilar, O. (2024). Potential Antifungal Effect of Copper Oxide Nanoparticles Combined with Fungicides against *Botrytis cinerea* and *Fusarium oxysporum*. *Antibiotics*, 13(3), 1–11. doi:10.3390/antibiotics13030215.
- [42] Gudkov, S. V., Burmistrov, D. E., Fomina, P. A., Validov, S. Z., & Kozlov, V. A. (2024). Antibacterial Properties of Copper Oxide Nanoparticles (Review). *International Journal of Molecular Sciences*, 25(21), 11563. doi:10.3390/ijms252111563.
- [43] Robinson, J. R., Isikhuemhen, O. S., & Anike, F. N. (2021). Fungal–metal interactions: A review of toxicity and homeostasis. *Journal of Fungi*, 7(3), 7 1–30. doi:10.3390/jof7030225.
- [44] Prasher, P., Singh, M., & Mudila, H. (2018). Oligodynamic Effect of Silver Nanoparticles: a Review. *BioNanoScience*, 8(4), 951–962. doi:10.1007/s12668-018-0552-1.
- [45] Hamidi, F., & Aslani, F. (2019). TiO<sub>2</sub>-based photocatalytic cementitious composites: Materials, properties, influential parameters, and assessment techniques. *Nanomaterials*, 9(10), 1–33. doi:10.3390/nano9101444.
- [46] Ramasamy, S., Singaraj, R., Jagadeesan, V., & Tamilarasan, N. (2024). The influence of ZnO nanoparticles on mechanical and early-age hydration behaviour of cement paste. *Matéria (Rio de Janeiro)*, 29(3), e20240068. doi:10.1590/1517-7076-rmat-2024-0068.
- [47] Jiang, Z., Zhang, B., & Yu, X. (2025). Photocatalytic Cement Mortar with Durable Self-Cleaning Performance. *Catalysts*, 15(3), 249. doi:10.3390/catal15030249.
- [48] Kozlova, I. V., & Dudareva, M. O. (2024). Methods of introducing a fine additive based on the TiO<sub>2</sub>–Bi<sub>2</sub>O<sub>3</sub> system into cement compositions. *Nanotechnologies in Construction*, 16(2), 90–99. doi:10.15828/2075-8545-2024-16-2-90-99.
- [49] Jiang, Z., Zhang, B., & Yu, X. (2025). Photocatalytic Cement Mortar with Durable Self-Cleaning Performance. *Catalysts*, 15(3), 1–14. doi:10.3390/catal15030249.